Latin American Journal of
Solids and Structures
www.lajss.org

Dynamic instability of imperfect laminated sandwich plates with in-plane partial edge load

Anupam Chakrabarti[a,*] and Abdul Hamid Sheikh[b]

[a]Department of Civil Engineering, Indian Institute of Technology, Roorkee-247667, Ph. +91(1332)285844, Fax. +91(1332)275568 – India

[b]School of Civil, Environment and Mining Engineering (Office: EM111), University of Adelaide, North Terrace, Adelaide, SA 5005 – Australia

Received 22 Jun 2010;
In revised form 22 Oct 2010

* Author email: anupam1965@yahoo.co.uk

Abstract

Dynamic instability of laminated sandwich plates having inter-laminar imperfections with in-plane partial edge loading is studied for the first time using an efficient finite element plate model. The plate model is based on a refined higher order shear deformation plate theory, where the transverse shear stresses are continuous at the layer interfaces with stress free conditions at plate top and bottom surfaces. A linear spring-layer model is used to model the inter-laminar imperfection by considering in-plane displacement jumps at the interfaces. Interestingly the plate model having all these refined features requires unknowns at the reference plane only. However, this theory requires C_1 continuity of transverse displacement (w) i.e., w and its derivatives should be continuous at the common edges between two elements, which is difficult to satisfy arbitrarily in any existing finite element. To deal with this, a new triangular element developed by the authors is used in the present paper.

Keywords

dynamic instability, imperfection, partial edge loading, sandwich plate, refined plate theory, Finite Element.

1 INTRODUCTION

The loads acting on parts of turbines, electric machines and parts of aircraft or ships due to aerodynamic and hydrodynamic effects are some typical examples of in-plane partial edge loads, which may induce dynamic instability. Dynamic instability of laminated sandwich plate subjected to in-plane partial edge loading is of considerable importance in mechanical, aerospace and many other engineering fields. The most important feature of laminated composite plates is that they are weak in shear compared to that of extensional rigidity. Due to this, the effect of shear deformation becomes very significant consideration for the analysis of such laminated structures. Moreover, the problem becomes much more complex if some inter-laminar imperfection is found in the form of weak bonding or otherwise. All these aspects have been discussed in detail in some earlier paper by the authors i.e., Chakrabarti and Sheikh [2].

Plates subjected to in-plane loads may lead to parametric resonance due to certain combination of the load parameters. The instability may occur below the critical load of the structure under in-plane loads over a range of excitation frequencies. The well-known Hill's method of infinite determinants is used for solving a system of Mathieu-type equation in the present problem to predict the stability properties. Dynamic instability of plates under different in-plane loads has been investigated by a number of different investigators in case of perfect interface. The dynamic stability of rectangular isotropic plates under various in-plane forces has been studied by Bolotin [1], Jagdish [10] and Yamaki and Nagai [16]. Hutt and Salam [9] and Deolasi and Datta [7] used finite element method based on first order shear deformation theory (FSDT) to study the parametric instability characteristics of thin isotropic plates. The dynamic stability of rectangular laminated composite plate due to periodic in-plane load is studied by Srinivasan and Chellapandi [14] using finite strip method (FSDT). Dynamic stability of laminated composite plates due to periodic in-plane loads is investigated by Chen and Yang [5] using FSDT. Dynamic instability of composite laminates has been studied by Kwon [11] (finite element method) and Chattopadhay and Radu [4] (analytical method) using Higher order shear deformation theory (HSDT). Lee [12] studied the finite element dynamic stability of laminated composite skew plates containing cutouts based on HSDT. Dynamic instability analysis of composite laminated thin walled structures has been carried out by Fazilati and Ovesy [8] by using two versions of FSM. Patel et al. [13] have done the parametric study on dynamic instability behavior of laminated composite stiffened plate by using the FSDT. Dynamic instability behavior of composite and sandwich laminates with interfacial slips has been studied by Chakrabarti and Sheikh [3] by using RHSDT (refined higher order shear deformation theory).

However, no studies based on RHSDT are found in the literature in case of imperfect laminated sandwich plates having in-plane partial edge loading. In this paper attempt has been made for the first time to study the dynamic instability of imperfect laminated sandwich plates with in-plane partial edge load using a finite element plate model recently developed by the authors based on RHSDT in combination with linear spring layer model. The problem is solved by finite element technique in order to have generality in the analysis and also to generate new results.

2 FORMULATION

Following the concept of refined higher order plate theory (RHSDT) and linear spring layer model discussed earlier, the through thickness variation of in-plane displacements (Fig. 1) may be expressed as follows.

$$\begin{aligned}\bar{u} =& u + \sum_{i=1}^{n_l} \left\{ \alpha_x^i \left(z - z_{i+1} \right) - \Delta u_i \right\} H\left(-z + z_{i+1} \right) + \\ &+ \sum_{i=n_l+1}^{n_l+n_u} \left\{ \alpha_x^i \left(z - z_i \right) + \Delta u_i \right\} H\left(z - z_i \right) + \beta_x z^2 + \eta_x z^3\end{aligned} \tag{1}$$

$$\overline{v} = v + \sum_{i=1}^{n_l} \left\{ \alpha_y^i \left(z - z_{i+1}\right) - \Delta v_i \right\} H\left(-z + z_{i+1}\right) + \\ + \sum_{i=n_l+1}^{n_l+n_u} \left\{ \alpha_y^i \left(z - z_i\right) + \Delta v_i \right\} H\left(z - z_i\right) + \beta_y z^2 + \eta_y z^3 \tag{2}$$

where $H(z - z_i)$ and $H(-z + z_{i+1})$ are the unit step functions.

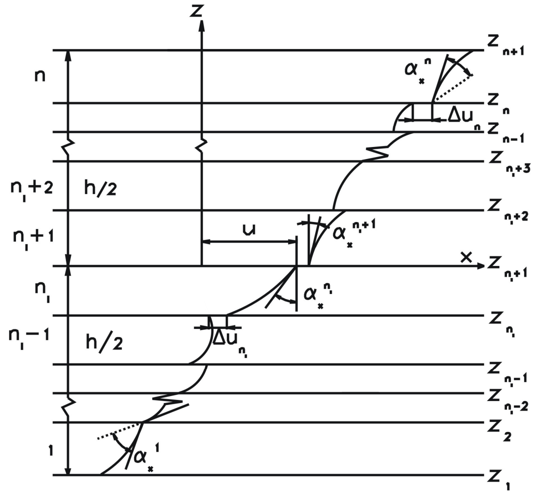

Figure 1 General lamination lay up and displacement configuration.

The transverse displacement is assumed to be constant over the plate thickness i.e.,

$$\bar{w} = w. \tag{3}$$

The stress-strain relationship of a lamina (say k-th lamina) in structural axes system $(x-y)$ may be expressed as

$$\left\{ \begin{array}{c} \sigma_x \\ \sigma_y \\ \tau_{xy} \\ \tau_{xz} \\ \tau_{yz} \end{array} \right\} = \left[\begin{array}{ccccc} \bar{Q}_{11} & \bar{Q}_{12} & \bar{Q}_{16} & 0 & 0 \\ \bar{Q}_{12} & \bar{Q}_{22} & \bar{Q}_{26} & 0 & 0 \\ \bar{Q}_{16} & \bar{Q}_{26} & \bar{Q}_{66} & 0 & 0 \\ 0 & 0 & 0 & \bar{Q}_{55} & \bar{Q}_{45} \\ 0 & 0 & 0 & \bar{Q}_{45} & \bar{Q}_{44} \end{array} \right] \left\{ \begin{array}{c} \varepsilon_x \\ \varepsilon_y \\ \gamma_{xy} \\ \gamma_{xz} \\ \gamma_{yz} \end{array} \right\} \quad \text{or} \quad \{\bar{\sigma}\} = \left[\bar{Q}^k\right] \{\bar{\varepsilon}\} \tag{4}$$

where the rigidity matrix $\left[\bar{Q}^k\right]$ can be formed with the material properties and fiber orientation of the k–th lamina following the usual techniques of laminated composites.

The imperfection at the k-th interface is characterized by the displacement jumps Δu_k (Fig. 1) and Δv_k, which may be expressed in terms of inter-laminar shear stresses at that interface utilizing the concept of linear spring-layer model as

$$\Delta u_k = R_{11}^k \tau_{xz}^k + R_{12}^k \tau_{yz}^k \tag{5}$$

and

$$\Delta v_k = R_{21}^k \tau_{xz}^k + R_{22}^k \tau_{yz}^k \tag{6}$$

where R_{11}^k, R_{12}^k, R_{21}^k and R_{22}^k are the compliance coefficients of the idealized linear spring layer at the k-th interface whereas τ_{xz}^k and τ_{yz}^k are the transverse shear stresses on that interface. Taking an adjacent layer of k-th interface, τ_{xz}^k and τ_{yz}^k may be expressed in terms of γ_{xz} and γ_{yz} (transverse shear strains) of that layer at this interface with the help of Eq. (4). Again Eqs. (1)-(3) may be used to express $\gamma_{xz} = \partial\bar{w}/\partial x + \partial\bar{u}/\partial z$ and $\gamma_{yz} = \partial\bar{w}/\partial y + \partial\bar{v}/\partial z$ where Δu_k and Δv_k will not fortunately appear and it will help to express Δu_k and Δv_k in terms of other terms easily. Now the condition of zero transverse shear stress/ strain at the top and bottom surfaces of the plate is utilized to express β_x, β_y, η_x and η_y as

$$\beta_x = -\frac{1}{2h}\sum_{i=1}^{n_l+n_u}\alpha_x^i,\ \ \beta_y = -\frac{1}{2h}\sum_{i=1}^{n_l+n_u}\alpha_y^i,\ \ \eta_x = -\frac{4}{3h^2}\left[w,_x - \frac{1}{2}\sum_{i=1}^{n_l}\alpha_x^i + \frac{1}{2}\sum_{i=n_l+1}^{n_l+n_u}\alpha_x^i\right]$$

and

$$\eta_y = -\frac{4}{3h^2}\left[w,_y - \frac{1}{2}\sum_{i=1}^{n_l}\alpha_y^i + \frac{1}{2}\sum_{i=n_l+1}^{n_l+n_u}\alpha_y^i\right]. \tag{7}$$

Finally, the condition of transverse shear stress continuity at the interfaces between the layers is imposed to express α_x^i and α_y^i in terms of the quantities at the reference plane as

$$\alpha_x^i = a_{xx}(\gamma_x) + a_{xy}(\gamma_y) + b_{xx}w,_x + b_{xy}w,_y$$

$$\alpha_y^i = a_{yx}(\gamma_x) + a_{yy}(\gamma_y) + b_{yx}w,_x + b_{yy}w,_y \tag{8}$$

where $\gamma_x (= w,_x - \theta_x = w,_x + \alpha_x^{n_l+1})$ and $\gamma_y (= w,_y - \theta_y = w,_y + \alpha_y^{n_l+1})$ are the transverse shear strains at the reference plane. The constants $(a_{xx}, a_{xy}, b_{xx}, b_{yy}, \ldots)$ found in the above equation are dependent on the material properties of the two layers adjacent to the i-th interface.

The FE formulation of the element has been described in detail in Reference [2]. The element developed may have any arbitrary triangular shape and orientation as shown in Fig. 2(a). It is mapped in a different plane $(\zeta - \eta)$ to have a regular shape as shown in Fig. 2(b).

The stiffness matrix $[k]$, geometric stiffness matrix $[k_g]$ and mass matrix $[m]$ are evaluated for all the elements and assembled together to form the overall stiffness matrix $[K]$, geometric stiffness matrix $[K_G]$ and mass matrix $[M]$ of the whole structure and these matrices are stored in a single array following the skyline storage technique. With these matrices, the equation of equilibrium for an elastic system undergoing small displacements at the instant of buckling may be written as

$$[M]\{\ddot{\partial}\} + [[K] - P[K_G]]\{\partial\} = \{0\}. \tag{9}$$

In the above equation, the in-plane load factor P is periodic and may be expressed in the form

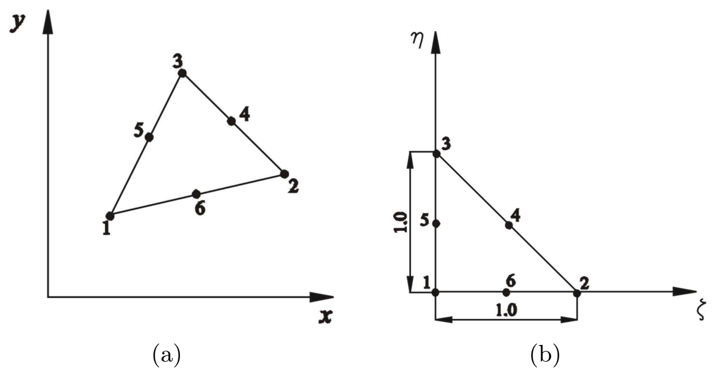

Figure 2 A typical element (a) before transformation (b) after transformation.

$$P = P_S + P_t \cos \Omega t \tag{10}$$

where P_S is the static portion of P, P_t is the amplitude of the dynamic portion of P with Ω as the frequency of excitation. The buckling load P_{cr} may be used to express P_S and P_t as follows:

$$P_S = \alpha P_{cr}, \quad P_t = \beta P_{cr} \tag{11}$$

where α and β are static and dynamic load factors respectively. Using Eqs. (10-11) the equation of motion (9) may be expressed as

$$[M]\left\{\ddot{\partial}\right\} + [[K] - \alpha P_{cr}[K_G] - \beta P_{cr}[K_G]\cos \Omega t]\{\partial\} = \{0\}\,. \tag{12}$$

Eq. (12) represents a system of second order differential equation with periodic coefficients of Mathieu-Hill type. One of the most interesting characteristics of the equation is that, for certain relationships between its coefficients, it has solution which is unbounded. The regions that correspond to the regions of dynamic instability is the physical problem under consideration in the present study. The boundaries of dynamic instability are formed by the periodic solution of period T and $2T$, where $T = 2\pi/\Omega$. The boundaries of the primary instability region with period of $2T$ are of practical importance and solution can be achieved in the form of trigonometric series:

$$\partial(t) = \sum_{k=1,3,5,\ldots}^{\infty} \left[\{a\}_k \sin\frac{k\Omega t}{2} + \{b\}_k \cos\frac{k\Omega t}{2}\right]. \tag{13}$$

After substitution of the above equation into Eq. (12), if the first term of the series is considered, it leads to a series of algebraic equations for the determination of instability regions. Principal instability region, which is of practical importance, corresponds to $k = 1$ and for this case the dynamic instability equation leads to

$$\left[[K] - \alpha P_{cr}[K_G] \pm \beta P_{cr}[K_G] - \frac{\Omega^2}{4}[M]\right]\{\Upsilon\} = \{0\}. \tag{14}$$

The two conditions under plus and minus signs correspond to two boundaries (upper and lower) of the dynamic instability region. Eq. (14) is solved by the simultaneous iteration technique proposed by Corr and Jennings [6]. The above eigenvalue solution give the value of Ω, which are the bounding frequencies of the instability regions for the given values of α and β. Before solving the above equations, the stiffness matrix $[K]$ is modified through imposition of boundary conditions. The boundary conditions used are same as discussed in some earlier studies [2].

3 NUMERICAL EXAMPLES

In this section some numerical examples are presented for imperfect laminated sandwich plates subjected to in-plane partial edge loading. Two different types of loading are considered. In loading type (I), the loaded length in the plate edge is near the corners (see Fig. 3(a)) while in loading type (II), the loaded length is in the middle of the edge (see Fig. 3(b)). In case of uni-axial loading the in-plane edge load is considered to be acting along the x-direction (Fig. 3). As there is no published result on dynamic instability of imperfect as well as perfect laminated sandwich plates subjected to partial edge loading, problem of a perfect isotropic plate subjected to uniform in-plane edge loading is presented for validation. The present results are found to be matching well in this case with the standard results. Subsequently in some cases the present results are compared with those obtained by using the FE package Abaqus (version 6.8). A number of new results are presented for imperfect laminated sandwich plates subjected to partial edge compression, which should be useful in future research.

3.1 Square isotropic plate simply supported at the four edges

To study the convergence and to validate the present results a square isotropic ($\nu = 0.3$) plate simply supported at all the edges having uni-axial in-plane uniform edge loading is analyzed by the present finite element model considering different mesh divisions (4x4, 6x6, 8x8, 12x12, 16x16 and 20x20). It is observed that the convergence in case of thin plate ($h/a = 0.01$) is obtained for mesh division 16x16. Hence all subsequent analyses are made taking mesh division: 16x16 for the higher thickness ratio (i.e., $h/a = 0.05$ and 0.20). The static load factor (α) and the dynamic load factor (β) are varied to identify the lower and upper boundaries of the excitation frequency. The values of the excitation frequency parameters, $\Omega = \omega a^2\sqrt{(\rho h/D)}$ obtained by using the proposed finite element plate model are presented in Table 1. The present results corresponding to thin plate ($h/a = 0.01$) are compared with the analytical results of Hutt and Salam [9]; and finite element (FSDT) results of Srivastava et al. [15]. The results are found to be matching well. Unfortunately there is no published result on the present problem for the thicker plates ($h/a \geq 0.05$). It may be observed that for a given α the difference between upper and lower excitation frequencies of the system increases with increase

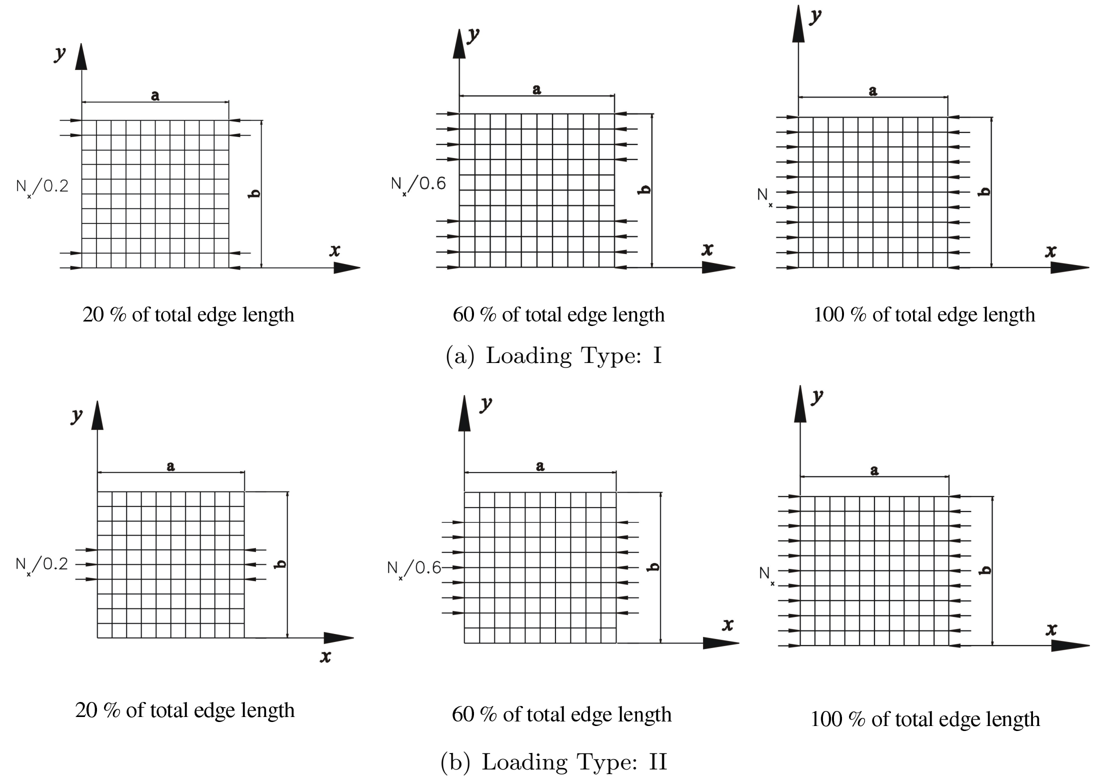

Figure 3 A rectangular plate (mesh size: $m \times n$) subjected to edge loading.

in the values of the dynamic load factor (i.e., β). This behavior is more prominent in case of thin plates.

3.2 Cross-ply square laminate simply supported at the four edges

The problem of a simply supported cross-ply (0/90/90/0) square laminate (Fig. 3, $a = b$) subjected to uni-axial in-plane partial edge loading is studied in this example. The analysis is carried out by the proposed element using mesh sizes (full plate) of 10x10 taking $h/a = 0.10$. In this problem, all the layers are of same thickness and material properties ($E_1 = 40E$, $E_2 = E$, $G_{12} = G_{13} = 0.6E$, $G_{23} = 0.5E$ and $\nu_{12} = 0.25$). The imperfections at the layer interfaces are defined by the parameters: $R^k_{11} = R^k_{22} = Rh/E$ and $R^k_{12} = R^k_{21} = 0.0$ where the non-dimensional parameter R is taken as 0.0, 0.5 and 1.0 ($R = 0.0$ represents perfect interface). In this paper some of the reported experimental values of imperfection parameters (R) are used, which generally varies from 0 to 1.0 or slightly higher. The loaded edge length (%) for both the load types are considered as 100 (i.e., fully loaded edge), 60 and 20 respectively, while α (0.0 to 0.6) and β (0.25 to 0.75) are varied to identify the lower and upper boundaries of the excitation frequency. The results obtained are presented in the form of excitation frequency parameter, $\Omega = \omega \frac{a^2}{h}\sqrt{\frac{\rho}{E}}$ in Table 2. Some of the present results ($R = 0.0$ and 100% in-plane edge loading)

Table 1 Excitation frequency parameters (Ω) for principal regions of instability of a simply supported square isotropic plate subjected to uniform in-plane edge loading (uni-axial).

h/a	β	References	Excitation frequency parameters, Ω					
			$\alpha = 0.0$		$\alpha = 0.20$		$\alpha = 0.35$	
			Upper	Lower	Upper	Lower	Upper	Lower
0.01	0.4	Present (4x4)	43.098	35.190	39.343	30.475	36.273	26.392
		Present (6x6)	43.167	35.246	39.406	30.524	36.331	26.434
		Present (8x8)	43.193	35.267	39.430	30.542	36.353	26.450
		Present (12x12)	43.213	35.284	39.448	30.556	36.369	26.463
		Present (16x16)	43.224	35.292	39.455	30.562	36.379	26.469
		Present (20x20)	43.224	35.292	39.455	30.562	36.379	26.469
		Hutt and Salam [9]	43.000	35.320	-	-	-	-
		Srivastava et al. [15]	43.160	35.370	-	-	-	-
	0.8	Present (4x4)	46.551	30.475	43.098	24.883	40.315	19.671
		Present (6x6)	46.626	30.524	43.167	24.923	40.374	19.703
		Present (8x8)	46.654	30.542	43.193	24.938	40.404	19.715
		Present (12x12)	46.676	30.556	43.213	24.949	40.422	19.724
		Present (16x16)	46.684	30.562	43.221	24.953	40.429	19.727
		Present (20x20)	46.684	30.562	43.221	24.953	40.429	19.727
		Hutt and Salam [9]	46.560	30.780	-	-	-	-
		Srivastava et al. [15]	46.540	30.730	-	-	-	-
	1.2	Present (4x4)	49.765	24.883	46.551	17.595	43.987	8.797
		Present (6x6)	49.845	24.923	46.626	17.623	44.057	8.811
		Present (8x8)	49.875	24.938	46.654	17.634	44.084	8.817
		Present (12x12)	49.899	24.949	46.676	17.642	44.104	8.821
		Present (16x16)	49.911	24.956	46.683	17.645	44.116	8.823
		Present (20x20)	49.911	24.956	46.683	17.645	44.116	8.823
		Hutt and Salam [9]	49.520	25.060	-	-	-	-
		Srivastava et al. [15]	49.540	24.020	-	-	-	-
0.05	0.4	Present (16x16)	42.841	34.980	39.108	30.293	36.056	26.235
	0.8	Present (16x16)	46.274	30.293	42.841	24.734	40.074	19.554
	1.2	Present (16x16)	49.469	24.734	46.274	17.490	43.724	8.745
0.20	0.4	Present (16x16)	38.222	31.208	34.892	27.027	32.169	23.406
	0.8	Present (16x16)	41.284	27.027	38.222	22.067	35.753	17.446
	1.2	Present (16x16)	44.135	22.067	41.284	15.604	39.010	7.802

are compared with the results obtained by using the FE software package Abaqus (version 6.8). The results obtained from the two sources compared well. In this case it is specifically observed that the excitation frequencies reduce rapidly in all the cases with increase in the values of imperfection parameters (R). This is the expected behavior because the stiffness of the plate reduces with increase in the values or R. Also the values of upper excitation frequencies obtained in case of Type: I loading are more compared to Type: II loading for $\alpha = 0.0$ while this is not so for higher values of α. The values of the lower excitation frequencies are always lesser in case of Type: II loading.

Table 2 Excitation frequency parameters (Ω) of a simply supported square laminated imperfect composite plate (0/90/90/0) subjected to uni-axial in-plane partial edge loading ($h/a = 0.10$).

R	Load type	Edge length (%)	β	Excitation frequency parameters, Ω					
				$\alpha = 0.0$		$\alpha = 0.3$		$\alpha = 0.6$	
				Upper	Lower	Upper	Lower	Upper	Lower
0.0	I	20	0.25	30.449	29.849	29.847	29.325	29.219	28.673
			0.50	30.693	29.692	30.101	29.057	29.484	28.391
			0.75	30.934	29.431	30.350	28.784	29.744	28.101
		60	0.25	31.455	28.866	28.306	25.243	24.568	20.760
			0.50	32.638	27.436	29.677	23.507	26.214	18.488
			0.75	33.758	25.896	30.962	21.589	27.731	15.828
	II	20	0.25	31.907	28.362	27.583	23.209	22.212	16.212
			0.50	33.499	23.361	29.483	20.614	24.618	12.032
			0.75	34.992	24.159	31.239	17.593	26.776	4.945
		60	0.25	32.021	28.262	27.446	22.931	21.914	15.872
			0.50	33.739	26.175	29.441	20.293	24.375	11.727
			0.75	35.372	23.903	31.306	17.253	26.606	4.789
	I/II	100	0.25	32.033	28.251	27.432	22.901	21.883	15.838
				31.983*	28.062*	27.155*	22.656*	21.612*	15.623*
			0.50	33.766	26.155	29.436	20.260	24.349	11.697
				33.483*	25.862*	29.055*	21.956*	23.012*	11.423*
			0.75	35.414	23.876	31.313	17.217	26.587	4.775
				35.112*	23.562*	31.057*	16.969*	26.323*	4.423*
1.0	I	20	0.25	17.207	16.397	16.225	15.311	15.113	14.009
			0.50	17.588	15.962	16.647	14.806	15.597	13.304
			0.75	17.954	15.503	17.050	14.252	16.051	11.917
		60	0.25	17.606	15.960	15.602	13.626	13.185	10.644
			0.50	18.353	15.044	16.478	12.487	14.256	9.060
			0.75	19.059	14.050	17.294	11.207	15.233	6.380
	II	20	0.25	17.722	15.834	15.423	13.138	12.624	9.605
			0.50	18.579	14.780	16.428	11.807	13.869	7.619
			0.75	19.387	13.630	17.365	10.286	14.998	4.825
		60	0.25	17.825	15.730	15.276	12.761	12.195	8.832
			0.50	18.783	14.568	16.387	11.293	13.565	6.525
			0.75	19.693	13.303	17.426	9.600	14.808	2.665
	I/II	100	0.25	17.830	15.725	15.269	12.747	12.180	8.816
			0.50	18.794	14.558	16.385	11.277	13.553	6.511
			0.75	19.712	13.290	17.430	9.584	14.799	2.658

*Values indicate results based on Abaqus (Version 6.8)

3.3 Simply supported square sandwich plate having three orthotropic layers

The dynamic instability of a simply supported three layered square plate ($h/a = 0.1$) subjected to in-plane uni-axial partial edge loading (Fig. 3) is studied here for both types of loadings (i.e., I and II, Fig. 3). The central orthotropic layer has a thickness of $0.8h$ while each of the face layers is $0.1h$ thick. The material properties of the orthotropic face layers are taken as multiple (K_t) of those of the central layer/core where the value of K_t is taken as 5.0. The material properties used for the core are E_{22}/E_{11} = 0.543, G_{12}/E_{11} = 0.2629, G_{13}/E_{11} = 0.1599, G_{23}/E_{11} = 0.2668, ν_{12} = 0.3. The imperfections at the layer interfaces are defined by the parameters: $R^k_{11} = R^k_{22} = Rh/E_{11}$ and $R^k_{12} = R^k_{21} = 0.0$ where the non-dimensional parameter R is varied from 0.0 to 1.2 (R = 0.0 represents perfect interface). The uni-axial in-plane partial edge loading is considered for both type I and type II loadings, while α and β are varied as before. The loaded edge length (%) for both the load types are taken as 100 (i.e., fully loaded edge), 60 and 20 respectively. The same loadings are also considered for all subsequent examples. The results obtained for the excitation frequency parameters, $\Omega = 100\omega\sqrt{(\rho h^2/E_{11})}$ are presented in Table 3. Some of the present results ($R = 0.0$ and 100% in-plane edge loading) are compared here also with the results obtained by using the FE software package Abaqus (version 6.8). The results are quite close to each other in all such cases. In the present case of sandwich plate, it is also observed that the values of both the upper and lower excitation frequencies reduce with increase in the values of imperfection parameter, R. But the rate of reduction is not as high as observed in case of the previous example of laminated composite plate. It is also found that with the increase in the values of loaded edge length the upper excitation frequencies always increase.

3.4 Square sandwich plate with laminated face sheets simply supported at the four edges

The problem of a square simply supported sandwich plate (0/90/C/90/0) having laminated face sheets subjected to in-plane partial edge loading (Fig. 3) is studied in this example for both types of loading (i.e., I and II, Fig. 3). The thickness of the core is $0.8h$ while that of each ply in the laminated face sheets is $0.05h$. Taking thickness ratio (h/a) of 0.20, the problem is solved for $\alpha = 0.0$, 0.3 and 0.6 while β is varied from 0.2 to 0.75. The non-dimensional excitation frequency parameters $\Omega = 100\omega a\sqrt{(\rho c/E_{11})}$ obtained for upper and lower boundary are presented in Table 4. The results show a consistent trend in their variation. The material properties of a ply in the laminated face sheets and those of core are as follows.

Face: $E_{11}/E = 40.0$, $E_{22}/E = 1.0$, $G_{12}/E = G_{13}/E = G_{23}/E = 1.0$, $\nu_{12} = 0.25$, $\rho_f = \rho$

Core: $E/E_c = 11.945$, $G_{c12}/E_c = G_{c13}/E_c = 1.173/6.279$, $G_{c23}/E_c = 2.415/6.279$, $\nu_{c12} = 0.0025$ and $\rho/\rho_c = 0.6818$. The imperfections at the layer interfaces are defined by the parameters: $R^k_{11} = R^k_{22} = Rh/E_c$ and $R^k_{12} = R^k_{21} = 0.0$ where the non-dimensional parameter R is varied from 0.0 to 1.0.

In this example of a thick plate ($h/a = 0.2$) it is observed that the difference between the lower and upper excitation frequencies are not so much as observed in the previous examples.

3.5 Sandwich plate under bi-axial in-plane partial edge loading

A square laminated sandwich plate (-45/45/C/45/-45) subjected to bi-axial in-plane partial edge loading (Fig. 3) is analyzed with boundary conditions SCSC i.e., two opposite edges (parallel to y: Fig. 3) simply supported and the other two edges clamped. The thickness and material properties of the core and the plies in the face sheet; and imperfection defined

Table 3 Excitation frequency parameters (Ω) for principal regions of instability of a simply supported sandwich plate having orthotropic layers subjected to uni-axial in-plane partial edge loading.

R	Load type	Edge length (%)	β	Excitation frequency parameters, Ω					
				$\alpha = 0.0$		$\alpha = 0.3$		$\alpha = 0.6$	
				Upper	Lower	Upper	Lower	Upper	Lower
0.0	I	20	0.25	15.951	14.876	14.648	13.420	13.154	11.681
			0.50	16.453	14.295	15.210	12.739	13.805	10.820
			0.75	16.935	13.678	15.744	11.998	14.414	9.830
		60	0.25	16.339	14.453	14.043	11.767	11.253	8.187
			0.50	17.199	13.403	15.045	10.433	12.496	6.068
			0.75	18.015	12.258	15.980	8.889	13.620	2.489
	II	20	0.25	16.327	14.466	14.062	11.824	11.320	8.310
			0.50	17.178	13.433	15.050	10.515	12.541	6.221
			0.75	17.985	12.307	15.973	9.000	13.646	2.613
		60	0.25	16.356	14.436	14.020	11.717	11.198	8.118
			0.50	17.236	13.371	15.038	10.372	12.453	6.002
			0.75	18.071	12.213	15.991	8.822	13.591	2.454
	I/II	100	0.25	16.362	14.430	14.012	11.698	11.178	8.090
				16.183*	14.162*	13.855*	11.456*	11.012*	7.923*
			0.50	17.247	13.360	15.036	10.348	12.437	5.975
				17.083*	13.162*	14.955*	10.058*	12.212*	5.723*
			0.75	18.089	12.196	15.995	8.794	13.581	2.439
				17.983*	12.062*	15.855*	8.656*	13.312*	2.323*
0.6	I	20	0.25	15.283	14.565	14.415	13.628	13.462	12.578
			0.50	15.624	14.186	14.785	13.207	13.871	12.094
			0.75	15.955	13.791	15.143	12.763	14.263	11.574
		60	0.25	15.792	14.010	13.623	11.479	10.997	8.132
			0.50	16.606	13.020	14.569	10.227	12.165	6.182
			0.75	17.379	11.941	15.454	8.785	13.224	3.095
	II	20	0.25	15.682	14.135	13.803	11.995	11.597	9.322
			0.50	16.397	13.288	14.617	10.969	12.567	7.899
			0.75	17.081	12.380	15.386	9.825	13.462	5.841
		60	0.25	15.828	13.974	13.572	11.348	10.848	7.872
			0.50	16.677	12.946	14.555	10.050	12.059	5.827
			0.75	17.484	11.827	15.475	8.552	13.158	2.387
	I/II	100	0.25	15.836	13.966	13.561	11.321	10.818	7.829
			0.50	16.692	12.930	14.552	10.015	12.037	5.782
			0.75	17.507	11.803	15.480	8.511	13.143	2.361

*Values indicate results based on Abaqus (Version 6.8)

Table 4 Excitation frequency parameters (Ω) of a simply supported square laminated imperfect sandwich plate (0/90/C/90/0) subjected to uni-axial in-plane partial edge loading (h/a = 0.20).

R	Load type	Edge length (%)	β	Excitation frequency parameters, Ω					
				$\alpha = 0.0$		$\alpha = 0.3$		$\alpha = 0.6$	
				Upper	Lower	Upper	Lower	Upper	Lower
0.0	I	20	0.25	22.756	22.217	22.105	21.516	21.391	20.703
			0.50	23.014	21.933	22.382	21.197	21.698	20.282
			0.75	23.267	21.638	22.651	20.852	21.991	19.680
		60	0.25	23.100	21.849	21.582	20.155	19.848	18.179
			0.50	23.682	21.171	22.238	19.371	20.601	17.243
			0.75	24.238	20.454	22.860	18.532	21.310	14.734
	II	20	0.25	23.242	21.698	21.369	19.601	19.220	17.134
			0.50	23.955	20.861	22.179	18.628	20.154	15.918
			0.75	24.635	19.972	22.946	17.580	21.032	11.891
		60	0.25	23.587	21.334	20.853	18.248	17.679	14.492
			0.50	24.633	20.108	22.036	16.789	19.068	12.579
			0.75	25.632	18.799	23.155	15.185	20.360	6.781
	I/II	100	0.25	23.661	21.256	20.741	17.949	17.336	13.875
			0.50	24.776	19.944	22.005	16.375	18.830	11.768
			0.75	25.843	18.541	23.200	14.633	20.213	6.568
0.5	I	20	0.25	15.472	15.209	15.155	14.879	14.822	14.525
			0.50	15.600	15.074	15.289	14.735	14.963	14.368
			0.75	15.725	14.935	15.420	14.586	15.101	14.202
		60	0.25	15.711	14.958	14.800	13.969	13.794	12.864
			0.50	16.067	14.558	15.190	13.525	14.226	12.359
			0.75	16.411	14.141	15.565	13.058	14.640	11.278
	II	20	0.25	15.783	14.883	14.694	13.696	13.485	12.356
			0.50	16.207	14.404	15.160	13.160	14.005	11.727
			0.75	16.616	13.903	15.608	12.593	14.501	10.029
		60	0.25	15.977	14.677	14.403	12.939	12.626	10.917
			0.50	16.588	13.980	15.080	12.139	13.396	9.941
			0.75	17.176	13.245	15.726	11.280	14.123	5.622
	I/II	100	0.25	16.026	14.626	14.330	12.745	12.404	10.533
			0.50	16.681	13.873	15.059	11.873	13.240	9.460
			0.75	17.312	13.077	15.756	10.933	14.027	4.212
1.0	I	20	0.25	12.504	12.204	12.143	11.823	11.757	11.410
			0.50	12.649	12.049	12.296	11.656	11.921	11.223
			0.75	12.791	11.889	12.445	11.482	12.080	11.023
		60	0.25	12.750	11.943	11.772	10.862	10.667	9.614
			0.50	13.128	11.510	12.193	10.366	11.146	9.023
			0.75	13.490	11.052	12.595	9.837	11.598	6.852
	II	20	0.25	12.811	11.878	11.681	10.622	10.395	9.152
			0.50	13.246	11.376	12.168	10.042	10.953	8.432
			0.75	13.663	10.844	12.632	9.417	11.478	4.464
		60	0.25	12.898	11.788	11.553	10.295	10.025	8.538
			0.50	13.417	11.191	12.132	9.603	10.689	7.683
			0.75	13.917	10.559	12.684	8.856	11.313	3.526
	I/II	100	0.25	12.924	11.760	11.514	10.191	9.906	8.331
			0.50	13.468	11.134	12.121	9.461	10.606	7.420
			0.75	13.991	10.469	12.700	8.669	11.262	3.489

at the layer interfaces are same as those used in the previous example. Taking the thickness ratio $(h/a) = 0.10$, static load factor (α) and dynamic load factor (β) are varied as in the previous examples. The excitation frequency parameters $\Omega = 100\omega a\sqrt{(\rho_c/E_{11})}$ obtained by the proposed FE model are presented in Table 5. In this example of bi-axial loading it may be observed that the values of the lower and upper excitation frequencies are closer compared to the other examples of uni-axial loading.

Table 5 Excitation frequency parameters (Ω) of square laminated imperfect sandwich plate (-45/45/C/45/-45) under bi-axial in-plane partial edge loading ($h/a = 0.10$).

R	Load type	Edge length (%)	β	Excitation frequency parameters, Ω					
				$\alpha = 0.0$		$\alpha = 0.3$		$\alpha = 0.6$	
				Upper	Lower	Upper	Lower	Upper	Lower
0.0	I	20	0.20	21.551	20.498	19.922	18.630	17.881	16.009
			0.60	22.508	19.304	21.038	17.028	19.304	12.550
			0.75	22.847	18.804	21.425	16.284	19.772	7.952
		60	0.20	21.703	20.344	19.613	18.010	17.108	14.939
			0.60	22.958	18.839	21.038	16.103	18.839	11.271
			0.75	23.406	18.223	21.539	15.250	19.424	7.055
	II	20	0.20	21.574	20.478	19.890	18.616	17.921	16.376
			0.60	22.580	19.270	21.038	17.178	19.270	14.512
			0.75	22.937	18.783	21.442	16.583	19.738	13.595
		60	0.20	21.811	20.230	19.381	17.526	16.499	14.144
			0.60	23.264	18.483	21.038	15.382	18.483	10.984
			0.75	23.782	17.772	21.621	14.467	19.161	8.234
	I/II	100	0.20	21.951	20.083	19.079	16.884	15.666	12.864
			0.60	23.668	18.016	21.038	14.338	18.016	9.120
			0.75	24.280	17.174	21.726	13.249	18.819	6.736
0.5	I	20	0.20	15.791	14.997	14.562	13.576	12.999	11.524
			0.60	16.509	14.092	15.405	12.332	14.092	8.704
			0.75	16.764	13.710	15.696	11.744	14.448	5.308
		60	0.20	15.918	14.868	14.302	13.052	12.341	10.593
			0.60	16.883	13.700	15.405	11.540	13.700	7.477
			0.75	17.228	13.219	15.792	10.848	14.156	4.310
	II	20	0.20	15.747	15.049	14.677	13.880	13.451	12.517
			0.60	16.394	14.288	15.405	12.998	14.288	11.435
			0.75	16.625	13.984	15.663	12.640	14.581	10.674
		60	0.20	16.006	14.774	14.108	12.643	11.824	9.921
			0.60	17.134	13.401	15.405	10.925	13.401	7.364
			0.75	17.534	12.838	15.859	10.184	13.935	5.929
	I/II	100	0.20	16.130	14.644	13.841	12.071	11.078	8.751
			0.60	17.488	12.987	15.405	9.985	12.987	5.448
			0.75	17.971	12.307	15.952	9.076	13.632	3.305
1.0	I	20	0.20	12.795	12.085	11.693	10.799	10.269	8.891
			0.60	13.433	11.268	12.451	9.651	11.268	6.227
			0.75	13.658	10.921	12.711	9.099	11.591	3.500
		60	0.20	12.892	11.988	11.497	10.403	9.775	8.209
			0.60	13.718	10.972	12.451	9.060	10.972	5.446
			0.75	14.012	10.550	12.783	8.439	11.369	2.947
	II	20	0.20	12.800	12.084	11.696	10.849	10.383	9.332
			0.60	13.453	11.286	12.451	9.880	11.286	8.026
			0.75	13.683	10.961	12.715	9.474	11.596	6.879
		60	0.20	12.976	11.898	11.313	10.016	9.282	7.544
			0.60	13.956	10.689	12.451	8.469	10.689	5.027
			0.75	14.304	10.189	12.847	7.788	11.161	3.162
	I/II	100	0.20	13.045	11.826	11.165	9.705	8.882	6.933
			0.60	14.158	10.462	12.451	7.970	10.462	4.072
			0.75	14.552	9.900	12.899	7.207	10.994	2.066

3.6 Simply supported double core rectangular sandwich plate with laminated stiff sheets

The problem of a simply supported rectangular sandwich plate having double core with three laminated stiff sheets (0/90/90/0/C/0/90/90/0C/0/90/90/0) is studied in this example taking uni-axial in-plane partial edge loading (Type I). The thickness of each core is $0.425h$ while that of each ply in the stiff laminated sheets is $0.0125h$. Their material properties and the imperfections at the layer interfaces are same as those used in the previous example. In this example, the plate subjected to uni-axial in-plane partial edge loading is analyzed with the proposed FE model with aspect ratio $(a/b) = 2.0$ and thickness ratio $(h/a) = 0.20$ for different values of imperfection parameter (R). In this example by varying α and β from 0 to higher values the full range of dynamic instability is studied. For all these cases, the excitation frequency parameter $\Omega = 100\omega a\sqrt{(\rho_c/E_{11})}$ obtained are presented in Figures 4–12. The figures (4-12) show the locations of the tips (i.e., $\beta = 0.0$) of the whole dynamic stability regions, which also shows the difference between the stability and instability regions It is observed from the results shown in the figures (4-12) that for higher values of α and β the uniform trend is disturbed in some cases.

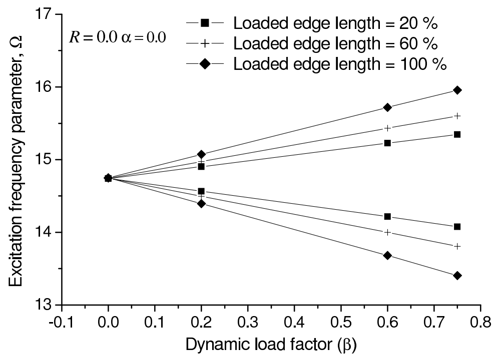

Figure 4 Instability region of a simply supported double core laminated sandwich plate ($R = 0.0$, $\alpha = 0.0$).

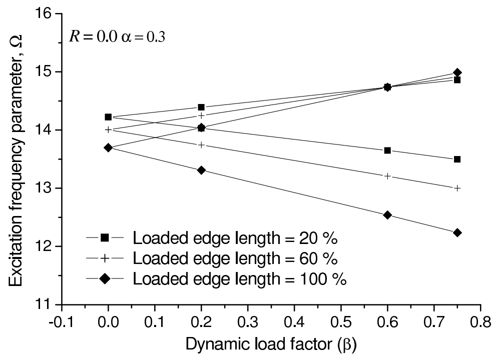

Figure 5 Instability region of a simply supported double core laminated sandwich plate ($R = 0.0$, $\alpha = 0.3$).

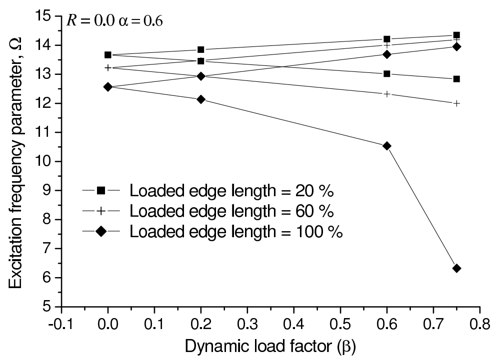

Figure 6 Instability region of a simply supported double core laminated sandwich plate ($R = 0.0$, $\alpha = 0.6$).

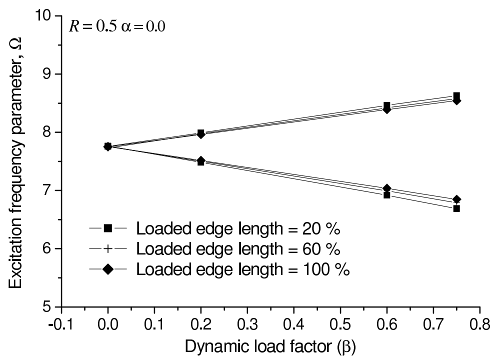

Figure 7 Instability region of a simply supported double core laminated sandwich plate ($R = 0.5$, $\alpha = 0.0$).

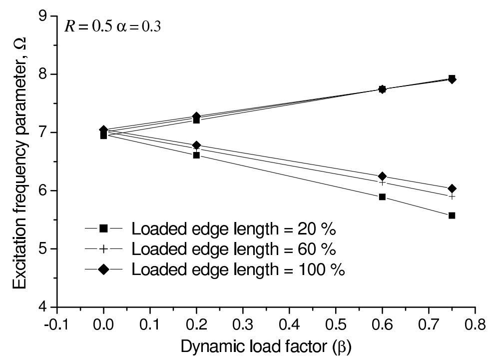

Figure 8 Instability region of a simply supported double core laminated sandwich plate ($R = 0.5$, $\alpha = 0.3$).

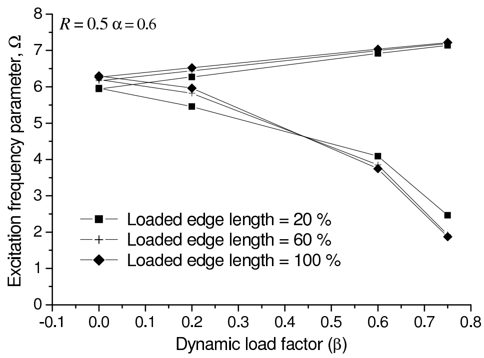

Figure 9 Instability region of a simply supported double core laminated sandwich plate ($R = 0.5,\ \alpha = 0.6$).

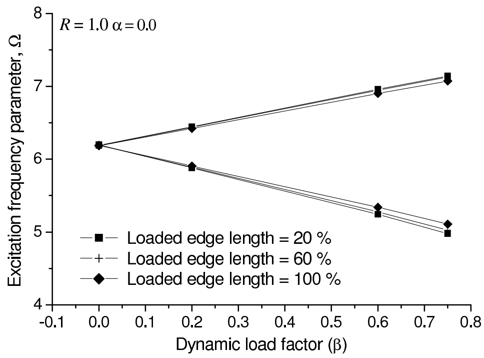

Figure 10 Instability region of a simply supported double core laminated sandwich plate ($R = 1.0,\ \alpha = 0.0$).

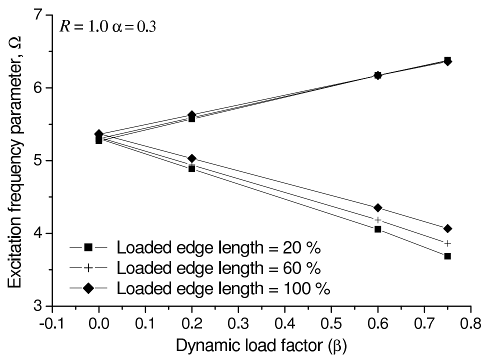

Figure 11 Instability region of a simply supported double core laminated sandwich plate ($R = 1.0,\ \alpha = 0.3$).

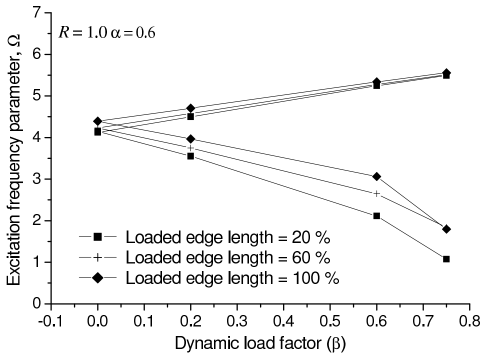

Figure 12 Instability region of a simply supported double core laminated sandwich plate ($R = 1.0$, $\alpha = 0.6$).

4 CONCLUSIONS

In this paper the dynamic instability characteristics of imperfect laminated sandwich plate subjected to in-plane partial edge loading is carried out by an efficient finite element plate model. The present finite element model has all the necessary features for an accurate modeling of the present problem while it is computationally as elegant as any single layer plate. As there is no investigation on dynamic instability of imperfect laminated sandwich plate using such a refined plate model, a number of problems are solved including different plate geometry, boundary conditions, stacking sequences, thickness ratio and other aspects. In general it may be observed that the dynamic instability region is more expanded in case of 100% (i.e. full) loaded edge length. Also with the increase in the imperfection parameter (R) the dynamic instability region is contracted and the effect of different loaded edge length is gradually reduced. In this process many results are generated, which should be helpful for future research.

References

[1] V. V. Bolotin. *The Dynamic stability of Elastic systems*. Holden-Day, San Francisco, 1964.

[2] A. Chakrabarti and A. H. Sheikh. Vibration of composites and sandwich laminates subjected to in-plane partial edge loading. *Comp. Sc. Tech.*, 67:1047–1057, 2007.

[3] A. Chakrabarti and A. H. Sheikh. Dynamic instability of composite and sandwich laminates with interfacial slips. *International Journal of Structural Stability and Dynamics*, 10(2):205–224, 2010.

[4] A. Chattopadhyay and A. G. Radu. Dynamic instability of composite laminates using a higher order theory. *Computer and Structure*, 77:453–460, 2000.

[5] L. W. Chen and J. Y. Yang. Dynamic stability of laminated composite plates by the finite element method. *Computer and Structure*, 36:845–851, 1990.

[6] R. B. Corr and A. Jennings. A simultaneous iteration algorithm for symmetric eigenvalue problems. *International Journal Numerical Methods Engineering*, 10:647–663, 1976.

[7] P. J. Deolasi and P. K. Datta. Parametric instability of rectangular plates subjected to localized edge compressing (compression or tension). *Computer and Structure*, 54:73–82, 1995.

[8] J. Fazilati and H. R. Ovesy. Dynamic instability analysis of composite laminated thin-walled structures using two versions of FSM. *Composite Structures*, 92(9):2060–2065, 2010.

[9] J. M. Hutt and A. E. Salam. Dynamic stability of plates by finite element method. *Journal of Engineering Mechanics ASCE*, 3:879–899, 1971.

[10] K. S. Jagdish. The dynamic stability of degenerate systems under parametric excitation. *Ingenieur-Archive*, 43:240–246, 1974.

[11] Y. W. Kwon. Finite element analysis of dynamic instability of layered composite plates using a high-order bending theory. *Computer and Structure*, 38:57–62, 1991.

[12] S. Y. Lee. Finite element dynamic stability analysis of laminated composite skew plates containing cutouts based on HSDT. *Composite Science & Technology*, 70(8):1249–1257, 2010.

[13] S. V. Patel, P. K. Datta, and A. H. Sheikh. Parametric study on the dynamic instability behavior of laminated composite stiffened plate. *Journal of Engineering Mechanics ASCE*, 135(11):1331–1341, 2009.

[14] R. S. Srinivasan and P. Chellapandi. Dynamic stability of rectangular laminated composite plates. *Computer and Structure*, 24:233–238, 1986.

[15] A. K. L. Srivastava, P. K. Datta, and A. H. Sheikh. Dynamic instability of stiffened plates subjected to non-uniform harmonic edge loading. *Journal of Sound and Vibration*, 262:1171–1189, 2003.

[16] N. Yamaki and K. Nagai. Dynamic stability of rectangular plates under periodic compressive forces. report of the institute of high speed mechanics. Technical report, Tohoku University, Japan, 1975.